**Atmospheric
Chemistry
and Physics
Discussions**

Atmospheric oxygen and carbon dioxide observations from two European coastal stations 2000–2005: continental influence, trend changes and APO climatology

C. Sirignano[1], R. E. M. Neubert[1], H. A. J. Meijer[1], and C. Rödenbeck[2]

[1]Centre for Isotope Research, University of Groningen, Nijenborgh 4, 9747 AG
Groningen, The Netherlands
[2]Max-Planck-Institute for Biogeochemistry, Hans-Knoell-Straße 10, 07745, Jena, Germany

ACPD

8, 20113–20154, 2008

**O$_2$ and CO$_2$
observations at
Lutjewad and Mace
Head 2000–2005**

C. Sirignano et al.

Title Page

Abstract	Introduction
Conclusions	References
Tables	Figures

◄◄ ►►

◄ ►

Back Close

Full Screen / Esc

Printer-friendly Version

Interactive Discussion

C. Sirignano et al.

Abstract

Seeking for baseline conditions has biased the carbon dioxide (CO$_2$) monitoring networks towards remote marine stations, missing part of the variability that is due to regional anthropogenic as well as land biota activity. We present here a five-year record of atmospheric CO$_2$ mixing ratios and oxygen/nitrogen ratios (O$_2$/N$_2$) from the coastal stations Lutjewad (LUT), the Netherlands and Mace Head (MHD), Ireland, derived from flask samples. Oxygen mixing ratios, concurrently measured with CO$_2$, help determine regional CO$_2$ fluxes by separating land fluxes from sea fluxes. Mace Head is the closest marine baseline station to Lutjewad, located at the same latitude, and therefore is taken as a reference. During the period of this study, we observed an average increase of CO$_2$ in the atmosphere of (1.7±0.2) μmol*(mol dry air)$^{-1}$ per year, and a change of the O$_2$ fraction of (−20±1) per meg per year. The observed acceleration of the oxygen decrease during the study period seems to confirm the existence of a net oxygen sink other than the combustion processes alone. The difference between the CO$_2$ summer minimum and the winter maximum is 14.4 μmol*(mol dry air)$^{-1}$ and 16.1 μmol*(mol dry air)$^{-1}$ at Mace Head and Lutjewad, respectively, while the opposite variation in the O$_2$ signal equals 113 per meg and 153 per meg, respectively. We also studied the APO (atmospheric potential oxygen) tracer at both stations. By this analysis, evidence has been found that we need to be careful when using APO close to anthropogenic CO$_2$ sources. It could be biased by combustion-derived CO$_2$, and models have to take into account daily and seasonal variations in the anthropogenic CO$_2$ production in order to be able to simulate APO over the continents.

1 Introduction

High-precision measurements of atmospheric oxygen concentrations have delivered important constraints for our understanding of the global carbon budget during the last almost twenty years (e.g. Keeling et al., 1993; Manning and Keeling, 2006). This is

possible as the global oxygen cycle is closely coupled to the global carbon cycle, with their concentration changes being anticorrelated for all but one major exchange mechanism: there is no mirroring oxygen-flux from the ocean to the atmosphere connected to the long-term uptake of CO_2 into the ocean by increased atmospheric CO_2 concentrations. This feature enables us to find an answer to the still open question: which fraction of the CO_2 produced by human activities is transferred into either of the two other reservoirs involved, the land biosphere or the world oceans. Building on this knowledge, we would like to know which processes are responsible for this partition, and how stable the ratio will be in the future. From production statistics and observations we know that only roughly half of the anthropogenic CO_2 stays in the atmosphere (IPCC, 2007). Both other reservoirs have strongly differing mean turnover times for CO_2, thus storing CO_2 for different periods of time before we have to account for its re-entrance into the atmosphere. That is why this partition ratio is required for climate projections. The knowledge about the effects and pathways of the anthropogenic perturbation of the natural carbon cycle is essential information in order to design effective policies and mitigation options aimed at minimizing anthropogenic climate change.

Through measurements of the decennial trends in both the atmospheric O_2 and CO_2 mixing ratios we can directly reconstruct the global budget of the two species (Keeling et al., 1996; Keeling et al., 1993; Bender et al., 1996; Keeling and Shertz, 1992; Battle et al., 2000). They also serve as constraints in multi-tracer inverse model simulations to study the spatiotemporal variability of those CO_2 sources and sinks (Le Quéré et al., 2003; Rayner et al., 1999; Bender et al., 1996). Apart from the trend, the seasonal variations of atmospheric O_2, can be applied to learn about the primary production in the oceans (Keeling and Shertz, 1992; Balkanski et al., 1999; Bender et al., 1996) or in general about seasonal patterns of oceanic processes causing fluxes at the air-sea interface and inter-hemispheric gradients (Keeling et al., 1998; Stephens et al., 1998; Battle et al., 2006; Garcia and Keeling, 2001).

CO_2 and oxygen have strongly differing seawater solubility, and, contrary to oxygen, CO_2 is involved in the oceanic carbonate-buffer system. Thus only a small portion of

Full Screen / Esc

Printer-friendly Version

Interactive Discussion

carbon within the Global Carbon Cycle of atmosphere, biosphere and oceans is airborne, but the majority of carbon is solved in the oceans. Also seasonal changes in the oceanic CO_2 content are largely buffered and thus not transferred into the atmosphere. The oceanic biology does not put a remarkable imprint on the atmospheric carbon cycle
5 when compared to the land biota. For oxygen the situation is just reversed. As the gas has a low solubility in water, seasonal variations in the seawater oxygen content are quickly transferred to the atmosphere, with a diffusion-controlled time-lag of 22 days (Keeling et al., 1993). This way the oceanic biology makes up for the biggest part of the annual oxygen concentration changes in the southern hemispheric atmosphere,
10 the total being very similar to the northern hemispheric annual fluxes where the land biosphere contributes much more to the total.

In order to quantify the coupling between the global oxygen and carbon cycles, the oxidative ratio (OR) is defined as the ratio of moles oxygen and carbon dioxide, concurrently exchanged in a given process, counted in the same transport direction, thus
15 rendering a positive number, i.e. $OR = \Delta\,mol\,O_2 : \Delta\,mol\,CO_2$. Plants, when photosynthetically producing oxygen, take up CO_2 from the atmosphere in a certain OR slightly larger than unity. The deviation from unity is due to the incorporation of elements other than carbon, that also need to be reduced from oxidized compounds. As plants produce material with different function and elemental ratios during their annual and life
20 cycles, the actual OR thus may vary. Land-use changes may even lead to changes in the global mean OR (Randerson et al., 2006). The built-up organic material will once be oxidized again, a process taking up oxygen and releasing CO_2 (and other oxidized elements). Fossil fuel combustion is using up oxygen for CO_2 production with an OR that also depends on the content of other oxidable elements apart from carbon. For
25 liquid and gaseous hydrocarbons, this is mainly determined by their hydrogen content. As for the possible extreme values we note that the oxidative ratio of pure carbon is 1, while the oxidative ratio of methane is 2, as with every molecule of CO_2 two molecules of water are formed. The generally used oxidative ratios are 1.95 for natural gas, 1.44 for liquid fuels and 1.17 for coal (Keeling, 1988).

O2 and CO2 observations at Lutjewad and Mace Head 2000–2005

C. Sirignano et al.

The fossil fuel mix of a country or region is mainly known from annual sales statistics, which until now introduces an unrealistic constancy in simulations, as compared to the actual combustion processes due to varying energy needs. Efforts are being made in order to describe and simulate the actual time-resolved and space-resolved fuel usage by defining major stationary as well as mobile users and their respective fuel consumption over time in weekly and annual cycles, on scales of kilometres and hours (Friedrich et al., 2006; Olivier and Berdowski, 2001). The energy demand of the Netherlands, where LUT station is located, is to a high degree satisfied by natural gas, due to large own natural gas reserves under the main land as well as under the North Sea, exploited since the early 1960s. This makes the country's fossil fuel mix unique with respect to its oxidative ratio.

A global carbon budget reconstruction needs long term observations at many stations to come to well-founded global mean values. Downscaling to a more regional assessment of the carbon budget needs a high resolution in the sampling sites' distribution, especially if one wants to infer the spatio-temporal distribution of the sources and sinks starting from concentration observations. The first records of atmospheric CO_2 concentration measurements were gained from whole-air flask samples (and later on-site continuous instruments), taken on remote, so-called clean-air stations with little continental and thus anthropogenic influence. Only in the 1990s more stations in the interior of the continents became operational, in order to study the rather undiluted biospheric and anthropogenic signals. In general the same strategy was followed when the measurement of the stable isotopologues of CO_2 ($^{13}CO_2$ and $CO^{18}O$), became more common. Again for oxygen concentration measurements, first the smoother marine background has been investigated, while the stronger but also more locally influenced signals at continental stations came into the picture nearly a decade later (Tans et al., 1989, 1990).

We present here the first five years of atmospheric O_2 and CO_2 mixing ratio measurements from whole air flask sampling at Lutjewad and Mace Head and subsequent analysis in the atmospheric laboratory of the CIO in Groningen.

O_2 and CO_2 observations at Lutjewad and Mace Head 2000–2005

C. Sirignano et al.

Title Page

Abstract	Introduction
Conclusions	References
Tables	Figures

|◄ | ►|
◄ | ►

Back | Close

Full Screen / Esc

Printer-friendly Version

Interactive Discussion

From the fossil fuel usage statistics and atmospheric CO_2 concentration observations we can expect a certain long-term decrease in the atmospheric oxygen concentration. After all, atmospheric O_2 disappears as it is transferred into CO_2. This slow process, as compared to the total abundance of oxygen, has been observed at many

5 places on Earth during the last decades (Bender et al., 1996; Keeling et al., 1996; Langenfelds et al., 1999; Manning and Keeling, 2006; Sturm et al., 2005b).

Atmospheric CO_2 and O_2 fields can be simulated using global or regional atmospheric transport models based on (re)analyzed meteorological data, with prescribed CO_2 and O_2 exchange at the Earth surface. While there are measurement-based CO_2

10 and O_2 flux data sets for the ocean, and temperature-dependent in- and outgassing of O_2 and N_2 is taken into account, the incorporation of the terrestrial biosphere mainly depends on biosphere models, carrying their own uncertainties. However, the contribution of the terrestrial biosphere can be removed from the measured data set as well as from the model results. For the models, just no biospheric contribution is taken

15 into account, the total signal is the sum of oceanic and combustion-derived fluxes. For the measured data this means that the variations in oxygen concentration are removed from the record as far as they are mirrored by changes in CO_2 concentrations (multiplied by the biospheric OR). This is equivalent to the introduction of the tracer APO (Stephens, 1999). For the measured data here the problem arises that fossil

20 fuel derived CO_2 cannot be distinguished from biospheric CO_2 production. The modelled APO can of course account for this fossil fuel contribution as an extra signal, but an erroneous estimate of the fossil fuel sources seasonal variability would again be able to mask a realistic prediction of the transport models. For clean air stations there should be no problem, as the actual fossil fuel contribution is generally low, however,

25 continental stations might suffer from the fact that the fossil fuel contribution is not handled correctly for the APO calculation. With the OR of the fossil fuel mix becoming higher, e.g. 1.7 on average in the case of the Netherlands, increasing errors would be introduced into the APO dataset. The O_2 and CO_2 observations at Lutjewad can be fundamental constraints especially in view of the final goal of establishing the CO_2

emission budget at a national level. All the results presented from Lutjewad are given as compared to Mace Head data, in order to highlight the different seasonal patterns and the gradients occurring between the two stations. Air flask samples taken periodically at Mace Head were analyzed at the CIO along with samples taken at Lutjewad. At Mace Head the dilution of the continental signals justifies the assumption that the APO seasonality is due mainly to oceanic processes such as solubility and the biological pump. The APO seasonal cycle characteristics of the two stations are reported here as well and compared to model expectations

2 Sampling stations and measurement techniques

With the goal of improving the temporal and spatial resolution of the O_2/CO_2 signal, for this study we chose Mace Head, Ireland (53° 20′N, 9° 54′W, 35 m a.s.l., operated by the Physics Department at the National University of Ireland, Galway), a marine boundary layer station on the west coast of North Western Europe as a European background monitoring site. The air samples were exclusively taken during Restricted Baseline Conditions (RBC, cf. Bousquet et al., 1996), i.e. during periods with wind directions within the sector from 210° to 290° and wind velocities higher than 4 m s^{-1}, or with wind directions within the sectors 200°–210° and 290°–300° and wind velocities greater than 8 m s^{-1}. Station Lutjewad, (53° 24′N, 6° 21′E, operated by CIO, University of Groningen), on the northern coast of the Netherlands and 30 km to the North-West of the city of Groningen (Fig. 1), at nearly the same latitude as MHD, serves as a continental station, also receiving "continental background" air with northerly winds (Neubert et al., 2005). We also use it as a special testcase for the incorporation of fossil fuel influences into carbon and oxygen cycle models as the fossil fuel OR is extraordinarily high. The station is equipped with a 60 m tall tower, with air intakes and basic meteorological equipments at different heights, and a research laboratory. Though located on the coast, this site is characterized by prevalent south-western and western winds, bringing air masses to the tower coming mainly from the north-western part of the

European continent. Air is collected from the top of the mast and carried to the laboratory where it is cryogenically dried and flushed through 2.5 l glass flasks fitted with two Louwers-Hapert high vacuum stopcocks, sealed with viton o-rings. The sampling process is remotely controlled by means of an automated system as described by Neubert et al. (2004). We avoided T-junctions, both in the sample collection and in the sample measurements systems, in order to prevent any fractionation due to pressure and temperature gradients (Stephens et al., 2007; Manning et al., 2001; Stephens et al., 1998; Sturm et al., 2005c).

Basic meteorological measurements at the station include:

– temperature, relative humidity and wind speed; at 7 m, 40 m and 60 m heights,

– wind direction (at 60 m),

– atmospheric air pressure and precipitation measurements.

For this study, one pair of air samples has been taken per week. The sampling time was usually in the afternoon hours, when the vertical atmospheric mixing is maximal. Originally, the flask pairs have been taken simultaneously, but starting from April 2004 onwards the flasks have been taken remote-controlled with one or two hours difference. Mace Head station is located in the County of Galway on Ireland's Atlantic coast. For a detailed description of the site and its location see Derwent et al. (2002). Samples have been taken under restricted baseline conditions as described by Bousquet et al. (1996), in order to sample just the North Atlantic air masses. The same kind of flasks as for Lutjewad has been used to collect air samples at Mace Head as well. Two samples were collected simultaneously every week if the RBC were met and logistics was permitting. The regular laboratory sample handling consisted of mass spectrometric oxygen-nitrogen ratio determination followed by a gas chromatographic analysis of the CO_2, CH_4 and CO mixing ratios. The atmospheric oxygen content was measured in relation to the N_2 content by a dual inlet isotope ratio mass spectrometer (DI IRMS),

a Micromass Optima, following a procedure adapted from Bender et al. (1994). Measurements of O_2/N_2 were made as the ratio of mass/charge (m/z)-numbers 32/28 on the main isotopologues of both gases, and compared to the ratio of a machine reference gas in order to derive a δ-value, expressed in per meg, with 1000 per meg being equal to 1‰ deviation of the ratios:

$$\delta_{\text{sample\_vs.\_mach.ref.}} = \left(\frac{\left(\frac{O_2}{N_2}\right)_{\text{SAMPLE}}}{\left(\frac{O_2}{N_2}\right)_{\text{mach.ref.}}} - 1 \right) \times 1000 \tag{1}$$

Each measurement consists of 16 consecutives switches between reference and sample inlet. Each switch was followed by 120 s idle time, before the actual signal was integrated for 30 s. Samples are measured in batches bracketed by standard measurements used for calibration purposes, as for the GC measurements, but in this case, we lack an internationally recognized oxygen mixing ratio scale. Therefore we express our results on our internal scale as defined by the primary whole air cylinder number "2534". Samples taken at Lutjewad or Mace Head have been measured in random order and alternating to each other during the entire period considered for this analysis. The $\delta O_2/N_2$ results referred to these two stations therefore belong to the same internally defined "CIO" oxygen scale. The introduction of a common scale is urgently required by the entire O_2 community (Worthy and Huang, 2005), and CIO is presently involved in different intercomparison exercises with one or more other institutions belonging to this community. The largest intercomparison programme the "GOLLUM" programme (Global Oxygen Laboratories Link Ultra-precise Measurements) (Miller, 2006), involves twelve institutes running high precision $\delta O_2/N_2$ measurements, with the final aim of being able to tie all the measurements to a common scale.

The concentrations of CO_2, as well as those of CH_4 and CO used to derive the APO, were measured by gas chromatography (HewlettPackard model 6890, adapted to the special requirements by D. Worthy, AES Environment Canada). CO_2 and CH_4 are separated using a 4 feet long Haysep Q packed column and detected by a Flame Ionization

Detector (FID), CO_2 after being converted to methane in a nickel-catalyst with hydrogen. For the separation of CO a different line is employed with a unibeads pre-column and a mol-sieve analytical column, another nickel catalyst methanizer for the conversion of CO to CH_4 and a FID. As the flasks are commonly filled to atmospheric ground level pressure to minimize permeation effects (Sturm et al., 2004), the flask air needs to be sucked through the GC inlet sample loops by a small membrane pump. A working standard, carefully calibrated against a set of World Meteorological Organization (WMO) standards (Zhao and Tans, 2006; and references therein), is measured after every two samples to normalize the analysis results. The CO_2 concentration is finally expressed as mole fraction and given in parts per million in dry air (ppm; equivalent to μmol*(mol dry air)$^{-1}$). At least a pair of target references, whose concentrations have also been calibrated on the WMO scale, is inserted in the measurement series, in order to check any occurring anomaly. The CIO laboratory is taking part in WMO CO_2 Round Robin exercises and the CarboEurope-IP intercomparison schemes.

3   Data selection

The O_2 and CO_2 concentration records at Lutjewad and Mace Head started routinely in 2000 and are shown in Fig. 2. Data have been first screened for suspected contaminated samples or locally influenced air samples, by removing all the samples with CO concentration above 300 ppb or CH_4 concentrations above 2000 ppb. Furthermore, at Lutjewad only samples taken between 8 h and 18 h, local time, have been selected, thereby excluding all kind of data collected for other purposes, such as intercomparison samples and diurnal cycles. Thereafter, an iterative procedure has been applied to eliminate the outliers from the prevailing data body. The iterative procedure consisted of two nested loops. An inner loop was aimed to find the best least square fit to the data. The fitting curve used is a linear combination of a harmonic series and a "weighted smooth" or "Loess" trend (Cleveland et al., 1990; Nakazawa et al., 1997; and references therein), according to the "general linear least squares" method (Press

et al., 1992). The harmonic series is the sum of the first three harmonics of the annual seasonal cycle, while the smoothing factor of the trend component has been chosen so that the time response was longer than a year. In the inner loop, the "de-trended" data (measurements minus the trend fit) were fitted with the seasonal component and the "de-seasonalized" data (measurements minus the harmonic series) with the trend component. This procedure was alternatively repeated, until no significant variation in the seasonal curve shape occurred. In the outer loop, the residuals between the measurements and the best fit were computed and those data, whose residual from the fit was larger than 2σ of the residuals' distribution, were excluded and considered anomalies. The retained data passed to the inner loop to be refitted again. The sequence was repeated until no further outlier was found.

4   Analysis, results and discussion

4.1 O_2 and CO_2 time series

Figure 2a and b show the CO_2 mole fraction at the two stations, while the O_2 records are given as $\delta O_2/N_2$ in panels 2c and d. The results of the data analysis are plotted representing the selected data as filled symbols, the anomalies as open symbols, the curve fit with three harmonics and the Loess trend as solid line, the Loess trend alone as thin solid line and an average linear trend as a dotted line. All the records show a significant seasonality with sharp summer passages and longer and flatter winter ones, typical for the northern location of the sites, characterized by a relatively short growing season. The parameters describing the seasonal pattern are listed in Table 1. For each species, we report the total amplitude of the fitting curve and the days of the year when the maxima and minima occur, as plotted in Fig. 2. The uncertainty associated with each parameter is based on a simpler fitting scheme with a linear component, instead of the Loess trend, and the periodicity represented just by the fundamental harmonic of the seasonal cycle. The uncertainties are then the standard errors of the fit parameters

Full Screen / Esc

Printer-friendly Version

Interactive Discussion

(Press et al., 1992). The remaining scatter of the data is the combination of measurement errors, residual local noise left in the filtered data set and the intrinsic variability of the signals themselves. At Lutjewad the CO_2 concentration has its minimum in the middle of August (around 14 August), and it increases towards the maximum around
5 7 March, mainly under the influence of terrestrial biosphere processes. The buffer capacity of the ocean and the thermal outgassing, which is in counter-phase with the marine biological activity dampen the seasonal variations of the CO_2 fluxes from and to the atmosphere, so that no ocean seasonality can be found in the CO_2 record. The ocean buffer does not affect O_2 exchanges at all; consequently, the oxygen sea-
10 sonality is given by the combination of both terrestrial and marine processes. Marine processes, however, show in the atmosphere a slower response to seasonal changes than the terrestrial ones. On the one hand, the system ocean-atmosphere shows a typical time lag of 22 days for O_2 between the response and the seasonal biological forcing that caused it. This is due to the presence of a finite air-sea interface and a not
15 infinite gas exchange velocity at this interface (Keeling et al., 1993). On the other hand, the atmosphere directly receives the fluxes occurring at the land interface. Therefore, the oxygen record mirrors the CO_2 oscillations, but with a delay caused by the influence of the marine biological fluxes superimposed to the land biota ones, as shown by both station's records. The Lutjewad O_2 minimum occurs around 28 March and the max-
20 imum on 11 September. The Mace Head record depicts similar patterns, with some phase lags, as the early winter CO_2 peak (on 26 February) or the later summer trough (on 27 August), that could be explained with a different origin of the terrestrial biospherical sources seen in the air masses sampled at Mace Head, compared to those of Lutjewad. The two stations, though located at the same latitude, sample different
25 kind of air masses, because of the sampling strategy and the wind distribution. In Lutjewad no distinct air-sampling selection has been applied, while samples at Mace Head have been taken under conditions aimed to sample just North Atlantic air masses, RBC (Bousquet et al., 1996). At Mace Head, the CO_2 record shows earlier and longer winter features and more abrupt change from winter to summer and vice versa, as compared

Back   Close

Full Screen / Esc

Printer-friendly Version

Interactive Discussion

to Lutjewad. As RBC strategy is meant to avoid the sampling of local air masses, the terrestrial signals here are derived from long-range transport and are representative of the average conditions along the 53rd degree of latitude. At Lutjewad, air masses with more local sources are sampled, in a region where the climate is mitigated by the effects of the Gulf stream. We can therefore speculate that this difference appears in the CO$_2$ record as if Lutjewad was located more to the south.

At Mace Head oxygen reaches its highest concentration around 8 September, almost simultaneously to Lutjewad, and has its minimum around 14 March, two weeks later. The CO$_2$ mixing ratio has in Lutjewad an annual peak-to-trough amplitude of $(16.1\pm0.4)\,\mu$mol*(mol dry air)$^{-1}$, while the annual δO$_2$/N$_2$ amplitude is (153 ± 3) per meg. The remoteness from land sources of Mace Head sampled air can be observed in our records in the dampening of both species' seasonal amplitude: $(14.4\pm0.2)\,\mu$mol*(mol dry air)$^{-1}$, peak-to-trough amplitude for CO$_2$ and (102 ± 5) per meg for O$_2$, due to the dilution of the signals through the atmospheric mixing. This dilution could also be due to different seasonal variations of the resp. atmospheric boundary layer heights, causing an enhanced "rectifier effect" in the records seen at Mace Head, as compared to those at Lutjewad. This dampening in the signals is even more evident when comparing them with those from two more continental stations like Puy de Dome in France and Griffin Forest in Scotland (Sturm et al., 2005a). Here, higher amplitudes than at Lutjewad or Mace Head have been recorded for both species. Peak-to-peak O$_2$ seasonal amplitudes have been reported to be 190 per meg and 171 per meg, at Puy de Dome ($45°\,46'$N, $2°\,58'$E, 1480 m a.s.l.) and from aircraft sampling above Griffin Forest ($56°\,37'$N $3°\,47'$W, 800 m a.s.l.), respectively. CO$_2$ peak-to-peak seasonal amplitudes are reported to be $18.2\,\mu$mol*(mol dry air)$^{-1}$ and $17.6\,\mu$mol*(mol dry air)$^{-1}$ for the two stations, respectively. Mixing phenomena occur also in the uplift of air masses as indicated by the shrink in the amplitudes reported for Jungfraujoch by Sturm et al. (2005b) compared to those we found at the two costal stations under investigation here.

4.2 Trends and interannual variability

The average trend (shown by a dotted line in Fig. 2) is derived from a fit through the selected data. The fitting curve has a series of the first three harmonics of the annual cycle, as seasonal component, but it has a linear trend component instead of the Loess one. In order to compare these average trends between the two stations, the same period, from July 2000 to July 2005, has been chosen for the fit. From this analysis it resulted that, at Lutjewad, CO_2 increased by $(1.7\pm0.2)\,\mu mol^*(mol\ dry\ air)^{-1}$ per year, while oxygen changed by (-20 ± 1.5) per meg per year. Comparable trends have been obtained for Mace Head: $(1.7\pm0.1\,\mu mol^*(mol\ dry\ air)^{-1}\ year^{-1}$ for CO_2 and (-19 ± 1.5) per meg $year^{-1}$ for O_2. These trends are mainly caused by human interferences on the natural cycles, such as combusting fossil fuels, that causes the atmospheric CO_2 level to rise and a proportional decrease of O_2. The O_2 trend shows a faster decrease compared to the trend observed at other sites for the previous years (Manning and Keeling, 2006; Prentice et al., 2001). The mean global annual oxygen decrease was 15.6 per meg per year from 1990 to 2000 (Manning and Keeling, 2006). The CO_2 trend seems also to have increased compared to the 1.51 $\mu mol^*(mol\ dry\ air)^{-1}$ per year average annual trend for the period 1990 to 2000 (Prentice et al., 2001), though the uncertainties on the estimates don't allow for a significant distinction. We can argue that both those trend accelerations seem to be consistent with an increased use of fossil fuel, especially because of the fast growing economy of the Far East countries (Raupach et al., 2007).

CO_2 and O_2 growth rates are highly variable from year to year as featured from the comparison between the linear and Loess trend. Unfortunately, the records presented here show the start up of the measurement series. They suffer from some data gaps and are still quite short if we want to precisely deduct the long term behaviour as well as characterize the interannual variability, in both growth rate and seasonal amplitudes. This data set is definitely not suitable for a year-to-year based analysis of the growth rate of the two species. Nevertheless, we can clearly detect differences between the

O_2 and CO_2 observations at Lutjewad and Mace Head 2000–2005

C. Sirignano et al.

two locations and show some peculiar variations in the trends of CO_2 and O_2 along the considered period. Figure 3 displays with dashed lines the average trend derived for the entire period (July 2000 to July 2005) as previously described, while solid lines represent the average trend derived in the same way, but for the period January 2002 to January 2005. Crosses represent the Loess component of the fit through the selected data points, as in Fig. 2. Gray tones are used for Lutjewad and black for Mace Head. In panel a, the results for CO_2 are presented, while in panel b those for O_2 are shown. All the trends are summarized in Table 2. In the period from January 2002 to January 2005 oxygen uptake seems to accelerate as compared to the average behaviour over the entire period. This behaviour can be noticed in the observations from both stations. No such acceleration can be observed for the airborne CO_2 mixing ratio measured at the two stations. If we would apply the budget equation method to derive sinks of anthropogenic CO_2, as in the following paragraph, we would derive a reasonable increase in the annual fossil fuel combustion from about $7.2\,\mathrm{PgC\,y^{-1}}$ to about $7.45\,\mathrm{PgC\,y^{-1}}$ according to Mace Head observations, but more than $9\,\mathrm{PgC\,y^{-1}}$, according to Lutjewad data. These regional estimates are extrapolated to global budget estimates (as in the paragraph Global carbon budget), with the land uptake as derived for the trend during the entire period 2000–2005. In both cases, the ocean uptake of anthropogenic carbon would have to almost double compared to the estimates based on the period 2000–2005. We regard this as not being realistic. Obviously, we require an extra O_2 sink until now not accounted for in top-down approaches used to reproduce the oxygen and carbon dioxide fluxes, following the anthropogenic disturbances. This extra sink, whatever its character might be, has then increased substantially around 2003. It is likely that this unaccounted sink resides in the terrestrial compartment as recently suggested by Randerson et al. (2006) and Cias et al. (2007). Furthermore, both articles agree that the OR associated to land processes need to be carefully reconsidered. Randerson et al. (2006) assert that it is no longer possible to define a univocal net terrestrial oxidative ratio associated to land biological processes, because of a global human-induced change in the plant coverage that is increasing the oxida-

tion status of the organic matter over time. The oxidative ratio associated to the CO_2 fluxes leaving the atmosphere is therefore now different from that related to the fluxes moving from land to the atmosphere, causing a disequilibrium forcing term to appear in the oxygen balance. As a consequence, a net oxygen sink has to be accounted for in proportion to the CO_2 source from the land ecosystems, such as heterotrophic respiration, according to the difference of those oxidative ratios. Ciais et al. (2007) have suggested the existence of another, up to now ignored, sink of atmospheric O_2. This additional oxygen sink is created by human-induced modification of the nitrogen cycle, starting from fertilizers production and their addition to croplands and ending with combustion of the fertilized organic matter and production of NO_x associated to fossil fuel burning. The first immediate effect is the subtraction of atmospheric oxygen because of industrial synthesis of ammonium nitrate fertilizer and because of the nitrification of the other forms of N-fertilizers occurring in the soil. However it is difficult to explain such an acceleration of the oxygen decrease of more than $1 \, \mu\text{mol}^*(\text{mol dry air})^{-1}$ per year by means of fluxes that though growing stay relatively small, adding up to no more than few tenths of $\mu\text{mol}^*(\text{mol dry air})^{-1}$ of O_2 sequestrated from the atmosphere each year. Even more challenging it would be to explain the extreme decrease of O_2 recorded inside the continent in the years 2003–2006, as reported for station Jungfraujoch by Valentino et al. (2008). This could be seen as a further evidence that the land processes are really playing a prominent role in the acceleration of the atmospheric oxygen decrease over time and it should be no random coincidence that this exteme uptake of O_2 occurs in years characterized by extreme summer events like in 2003 (Ciais et al., 2005).

Another evident feature in Fig. 3 are the gradients between Mace Head and Lutjewad. In January 2003, CO_2 was $3 \, \mu\text{mol}^*(\text{mol dry air})^{-1}$ lower and O_2/N_2 26 per meg higher at Mace Head than at Lutjewad. Probably, this gradient can be explained as a result of the dilution of the signals of the anthropogenic processes, as moving away from the continents toward remote marine areas, where just oceanic air masses are sampled. As final remark, we can also notice that both CO_2 and $\delta \, O_2/N_2$ gradients

tend to increase in the last few years.

4.3 Global carbon budget

Based on long term trends of oxygen and carbon dioxide, as shown first by Keeling et al. (1996), it is possible to estimate the partitioning of the anthropogenic CO_2 fluxes from the atmosphere to the oceans and the terrestrial biosphere, by simultaneously solving the budgets for the airborne CO_2 (Eq. 2) and O_2 (Eq. 3) fractions.

$$CO_2 = (CO_2)_{bg} + F + B + O \tag{2}$$

$$O_2 = (O_2)_{bg} - \phi \times F - \beta \times B + Z \tag{3}$$

The airborne carbon dioxide and oxygen contents (CO_2 and O_2 in the budget equations, respectively) can be broken down into their different components: an atmospheric background (indicated by the subscript bg), the CO_2 released (F) and O_2 used ($-\phi \times F$) due to anthropogenic processes, the biosphere carbon (B) from all biological processes occurring on land and the amount of oxygen moved in the opposite direction by the same kind of processes ($-\beta \times B$) and, finally, the amount of carbon from oceanic processes (O) uncorrelated with the amount of oxygen exchanged at the ocean interface (Z). We defined ϕ and β as the oxidative ratios (O_2/CO_2) obtained from the stoichiometry of the reactions involving the two molecules; ϕ for fossil fuel and β for biospheric processes. After derivation w.r.t. the time we compare the expected total CO_2 release and O_2 usage due to anthropogenic processes to the measured changes of the airborne CO_2 and O_2 molar ratio ($\frac{d}{dt}CO_2$ and $\frac{d}{dt}O_2$). The differences are then apportioned in order to calculate the biospheric ($\frac{d}{dt}B$, Eq. 4) and oceanic ($\frac{d}{dt}O$, Eq. 5) carbon sinks. We assume that secular ocean CO_2 uptake leaves the atmospheric O_2 concentration unchanged, but a constant rate of atmospheric O_2 increase of $(0.2 \pm 0.2)\,\mu\text{mol}^*(\text{mol dry air})^{-1}\,\text{year}^{-1}$ can be assigned to the O_2 net outgassing from the ocean ($\frac{d}{dt}Z$, Manning and Keeling, 2006), in order to take into account the global ocean warming (Levitus et al., 2000). As all the components are intended as

Title Page

Abstract	Introduction
Conclusions	References
Tables	Figures

|◄ | ►|

◄ | ►

Back | Close

Full Screen / Esc

Printer-friendly Version

Interactive Discussion

molar fractions of dry air, the term Z is also used to account for the different solubility of N_2 and O_2 in water, and the consequences for the atmospheric ratio due to ocean warming. This term is equivalent to the term Z_{eff} in Manning et al. (2006).

We solve the budget equations according to the O_2 and CO_2 data extrapolated from the trend registered at our two stations on 1 January, each year from 2000 to 2006, deriving the oceanic and terrestrial CO_2 uptake according to the following equations:

$$\frac{d}{dt}B = \frac{d}{dt}CO_2 - \frac{d}{dt}F - \frac{d}{dt}O \tag{4}$$

$$\frac{d}{dt}O = -\left(\frac{\Phi}{\beta} - 1\right) \times \frac{d}{dt}F + \frac{d}{dt}CO_2 + \frac{\frac{d}{dt}O_2 - \frac{d}{dt}Z}{\beta} \tag{5}$$

Anthropogenic CO_2 release data before 2002 have been taken from Marland et al. (2005), the emissions for the remaining years until 2006 have been estimated assuming a proportional global increase of emission rate equal to 3% per year, as reported by Raupach et al. (2007). This caused an average emission rate of $(3.4\pm0.2)\,\mu\text{mol}^*\,(\text{mol dry air})^{-1}\,CO_2\,\text{year}^{-1}$. The stoichiometric factor $\phi=1.4\pm0.1$ has been obtained as the weighted average of the oxidative ratios reported by Keeling (1988), for the four main fossil fuel categories: natural gas, crude oil and natural gas liquids, coal, and natural gas flaring. The weights are the fractions of the total emissions, as derived from the statistics of the global anthropogenic CO_2 emissions for the period 2000–2004 (Raupach et al., 2007), assuming an uncertainty of each fossil fuel fraction of 5%. Fuel emissions from "international bunkers", reported to be about 4% of the total industrial CO_2 emissions (Raupach et al., 2007), have been added to the category crude oil and natural gas liquids for the oxidative ratio calculation. The factor $\beta=1.1\pm0.05$ has been taken from Severinghaus (1995). We use the factor 0.471 to convert PgC to $\mu\text{mol}^*(\text{mol dry air})^{-1}$ and 4.8 to convert $\mu\text{mol}^*(\text{mol dry air})^{-1}$ to per meg (Battle et al., 2000). Using Mace Head data, we found that from the $(7.2\pm0.4)\,\text{PgC year}^{-1}$ anthropogenic carbon, released per year on average during 2000–2006, $(3.6\pm0.2)\,\text{PgC year}^{-1}$ remains airborne, $(2.5\pm1.8)\,\text{PgC year}^{-1}$ is taken up

by the oceans and thus the rest, being (1.1±2.4) PgC year^{-1}, by land biota. The Lut-
jewad data are more influenced by continental sources and sinks and therefore they
are less suited to depict the baseline conditions necessary to reconstruct the global
budget. Still, the findings from the Lutjewad observations are quite similar to those
5 from Mace Head, with an oceanic sink of (2.9±2.1) PgC year^{-1} and a land sink of
(0.8±2.8) PgC year^{-1}. As compared to the budget solutions for the 1990s, given by
Manning and Keeling (2006), the annual atmospheric CO_2 increase we find is slightly
larger than the 3.2 PgC year^{-1} they report, as a consequence of the fact that fossil fuel
usage has indeed increased over the recent years, making anthropogenic emissions in-
10 crease from 6.3 PgC year^{-1} in the 1990s (Prentice et al., 2001) to (7.2±0.4) PgC year^{-1}
from January 2000 to January 2006.

    The kind of calculation above assigns the role of compensating the increased amount
of anthropogenic carbon entirely to the ocean sinks. The budget solutions derived for
the period 1990 to 2000 by Manning and Keeling (2006), from the observations of the
15 Scripps atmospheric sampling network are: 1.41 PgC year^{-1} and 1.71 PgC year^{-1} for
the land and ocean sinks, respectively. Our results show the ocean sink increasing
by more than 1 PgC year^{-1}. Accounting for extra sinks of atmospheric O_2 alone due
to land use change (Randerson et al., 2006) or due to land nitrogen processes (Ciais
et al., 2007), would definetely decrease our large ocean sink. While this would be
20 more plausible than the large ocean sink, it is unclear why the suggested alternative
mechanisms (Ciais et al., 2007; Randerson et al., 2006) would suddenly become so
much more important between 2002 and 2004. The anomalously hot summer of 2003
in Europe, or the recovery period directly afterwards, might be the cause of new, even-
tually temporary O_2 sink mechanisms. However, the relation between the hot and dry
25 summer months of that year, and the mechanisms suggested by Ciais et al. (2007) and
Randerson et al. (2006) is yet unclear.

4.4 Effects of fossil fuel emissions on APO trend and climatology

The oceanic component of the seasonal atmospheric oxygen fluxes can be calculated by removing the assumed terrestrial component from the oxygen record. Following the definition of Stephens et al. (1998) APO is a tracer sensitive to ocean-atmosphere exchange of O_2 and CO_2, but not to biospheric O_2/CO_2 exchanges. Therefore, it is applied to describe the seasonal variation due to the processes that occur at the air-sea interface. If we assume that the seasonal variation of the atmospheric CO_2 mixing ratio is merely due to the terrestrial processes, then the terrestrial component of the oxygen signal can be removed by subtracting the amount of oxygen that has been used to produce the observed variation of the atmospheric carbon content. In this case, the observed variation of atmospheric carbon content is multiplied by the factor $\beta=1.1$, before adding it to the observed variation in the oxygen content. The factor 1.1 is the oxidative ratio generally associated with the terrestrial biological processes, i.e. photosynthesis and respiration as a whole, as derived by Severinghaus (1995). In this definition, CO_2 is the atmospheric carbon content, or total atmospheric carbon (TAC), as originally introduced by Stephens et al. (1998); it includes also the contribution of CH_4 and CO and accounts for oxygen used to oxidize these species to CO_2 as well. Substituting the airborne CO_2 and O_2 with their different components reported in the budget Eqs. (2) and (3), the APO definition can be expressed in terms of variations from an arbitrary offset as follows:

$$\Delta APO = \Delta O_2 + \beta \times \Delta CO_2 = \Delta Z + \beta \times \Delta O - (\phi - \beta) \times \Delta F \tag{6}$$

Here the term $(\phi - \beta) \times \Delta F$ is the residual of the terrestrial processes that is not removed. This residue is usually assumed to be of no or small influence when considering the seasonal variation of APO. For marine background stations the mixing processes are supposed to have smoothed and diluted the seasonal variations and the fuel mix variations of the fossil fuel emission very close to insignificance, and the difference $(\phi - \beta)$ is then only 0.3, ϕ being taken as 1.4. However, this assumption cannot be used when dealing with continental or continentally influenced records. The anthropogenic CO_2

Full Screen / Esc

sources are too close to be able to assume an efficient dilution of their signals or even a smoothing of their annual variability. Furthermore, ϕ can be different from the global mean of 1.4 under local conditions and, for example, in regions with high methane consumption it can get closer to two, enhancing the influence of any variation of an-
thropogenic CO_2 emissions on APO. Finally, due to increased use of fertilizer in the agriculture since industrialization, the oxidative ratio β has been proposed to become as small as 0.76 (Ciais et al., 2007). All these factors add an extra, not accounted for, negative trend to the APO series that does not belong to any oceanic process. They have the effect of modifying the APO climatology because of the residual signal
of fossil fuel combustion, and even of terrestrial biospheric signals, if the value of β is variable, introducing additional seasonal variability to the tracer, due to this spurious anthropogenic contribution. When comparing observations with model runs, this extra variability could then be interpreted as a misrepresentation of the reality by the applied transport models.

The APO records for Lutjewad and Mace Head have been calculated using the data selected with the procedure described in the paragraph "data selection". Therefore only the data selected to be regionally representative for both CO_2 and O_2 have been chosen. The contribution to the total carbon of CO and CH_4 has also been accounted for by adding the term $(\beta-2)\times\Delta CH_4+(\beta-0.5)\times\Delta CO$, to each of the selected data points.
An offset represented by the value at the time 2000.0 of their linear trend has been subtracted from the data in order to express APO variations in a comparable way for both observations and model estimates. The resulting time series have been fitted with a linear combination of the first harmonic component and a linear trend and are presented in Fig. 4, where the samples are plotted as black full circles and the fit curves appear
as black solid lines. The observations have been compared to model forecasts based on surface flux fields transported by applying the TM3 atmospheric transport model with a spatial resolution of 1.8×1.8 degrees. Surface fluxes for oceanic CO_2, term O in Eq. (6), were taken from the $dpCO_2$-derived data set by Takahashi et al. (2002) patterns, with long-term mean fluxes taken from the inversion of ocean interior data by

Gloor et al. (2001). Ocean oxygen, term Z in Eq. (6), is based on the flux climatology by Garcia and Keeling (2001) patterns, with long-term fluxes by Gruber et al. (2001). Anthropogenic CO_2 estimates (F) were based on the emissions reported by the Emission Database for Global Atmospheric Research (EDGAR) (Olivier and Berdowski, 2001) augmented with diurnal, weekly, and seasonal variations (in addition to the interannual variations), and extrapolated to recent years based on BP statistics (BP, 2008). As the measurements show the variation of oxygen compared to nitrogen, the model has been corrected for the N_2 influence present in the measured APO signal due to N_2 in-gassing and outgassing of the oceans, adding a term derived from simulations based on N_2 fluxes from the OPA ocean biogeochemical model by Le Quéré et al. (2007; and references herein). The model data used in this study come from a simulation dataset starting from 1995 and ending in 2006, having six-hourly resolution. For each air sample the corresponding model result has been looked up and used, simulated for the same day and time range as the physical air sample. Furthermore, in analogy with the observed data, an arbitrary offset has first been derived for each component, by extrapolating the linear trend through all data at the time 2000, and then this offset has been removed from the data series of that component. These variations of the different atmospheric components have been used to calculate the modelled APO variation, as in the last term of Eq. (6). In the plots of Fig. 4, model outputs are presented as grey plus-signs and the fitting curves are drawn as dashed lines. Panel a refers to Lutjewad and panel b refers to Mace Head. The parameters characterising the fitting curves are summarized in Table 3; in particular, the trend values refer to the curves in Fig. 4, while the peak-to-trough amplitudes and phases refer to the more accurate evaluation obtained by average detrended data shown in Fig. 6. The results are expressed as μmol/mol dry air, representing the variation from the beginning of year 2000 of the tracer APO in standard dry air, containing 20.95% of O_2; therefore, the factor 1/0.2095 is used to convert the quantities from (μmol/mol dry air) to per meg. Being at the same latitude both on the North Atlantic Ocean, Lutjewad and Mace Head were expected to show comparable APO behaviour, as confirmed by the comparable model predictions.

However, the observations demonstrate a larger amplitude and a steeper slope at Lutjewad than both the model predictions and the Mace Head observed record show. This could be the result of smaller rectifying effects above this area than at Mace Head, that the model fails to reproduce. It is, however, more likely that both these features are caused by the fact that the fossil fuel influence on Lutjewad record is different from what is assumed in Eq. (6), and the model fails to reproduce properly its seasonal variability. First of all, the term $(\phi - \beta) \times \Delta F$, due to the differing oxidative ratios of biospheric processes and fossil fuel combustion, could be larger than assumed in first instance, causing the steeper slope. Lutjewad station receives air coming directly from the continent, with a higher – and presumably not yet well-mixed – fossil fuel CO_2 load. In most of the countries of Western Europe, most pronouncedly so the Netherlands, natural gas plays a dominant role, causing ϕ to be higher than 1.4 and consequently causing $(\phi - \beta)$ to be higher than the assumed 0.3. Furthermore, as natural gas is mainly used for energy purposes, among them house heating and electricity production, they are subject to variable seasonal demands, that cause a larger uptake of O_2 from the atmosphere in winter than in summer in N.W. Europe. Therefore not only the total fossil fuel usage, but also the oxidative ratio associated to it is influenced by seasonal variations, as the demands of all other kinds of fuel stay more or less the same throughout the whole year. This process occurs in phase with the oceanic O_2 uptake; therefore the APO amplitude experiences a deepening of the winter trough, hence an increase of the amplitude. So, observing both Fig. 4 and Table 3, we can summarise by saying that the model can realistically reproduce the observations at Mace Head, but it shows clear deficits for Lutjewad. When we investigate the mean difference between observed and modelled data as a function of $(\phi - \beta)$, this mean difference is $-3.29\,\mu$mol O_2/mol dry air when we put in the usual value of 0.3 for $(\phi - \beta)$. Enlarging $(\phi - \beta)$, as might be realistic for the situation in the Netherlands, the difference gets more positive and in a linear way becomes zero when $(\phi - \beta)$ is equal to 0.64 and thus ϕ would be equal to 1.74. This finding agrees very well with the annual average OR of 1.69±0.06 derived from the peculiar Dutch fuel mix estimate, based on quarterly records of fossil fuel con-

sumption in the Netherlands as reported by Meijer et al. (1996) and summarised in the plot of Fig. 5. Here the variation during one typical year of fuel consumption is shown, bunched in the three main categories solid, liquid and gas. The resulting oxidative ratio and its behaviour during the year as represented in Fig. 5 has been calculated by assigning an average oxidative ratio of 1.17, 1.4 and 1.95 respectively to each of the three fuel categories, solid, liquid and gas as in Keeling (1988). The detrended observational data have been merged by month of the year. For Mace Head, given the scarcity of data points they have been merged every two months to make each point more representative of the whole time range. The selected model outputs were detrended and fitted in the same way as the observations. The APO seasonality is thus shown in Fig. 6a (Lutjewad) and b (Mace Head). The first six months' averages have been repeated for a better clarity of the representation. The harmonic fit peak-to-trough amplitudes and phases are reported in Table 3. Looking at the climatology of both APO records we can notice similar features, as well, among which a very peculiar one is the presence of a second higher relative maximum during the months in early autumn, following the one in early summer, as highlighted by a second curve fit through the Mace Head APO climatology data. This last curve contains also a second harmonic component together with the fundamental one of the seasonal cycle, with the purpose to follow more closely the data. We suggest that the first maximum is mainly an effect of the increase of marine primary production, following the increased availability of light in phase with nutrient availability. The second peak occurs in coincidence with the highest surface temperatures, and therefore could be caused by thermal outgassing in response to the decrease in the gas solubility following the increase in temperature. Comparing the model curves, especially at Lutjewad, shows that the seasonal variation in the fossil fuel emission is important even when evaluating APO, which should be strictly representative of marine processes alone. Assuming that the fossil fuel component of the APO tracer has the variability of its source, we have taken estimates of the fossil fuel contents which don't account for seasonal or diurnal variation (i.e. simply based on EDGAR statistics) and we have modulated them according to the curve of

the total quarterly C emissions. Furthermore, we have tuned also the factor ϕ in that equation according to the OR curve representing its annual Dutch behaviour, taking 1.69 as the average value. In this way, we obtain an extreme estimate of a seasonally variable strength of the fossil fuel term, F in Eq. (6), that we define as model-modified output. This representation of the fossil fuel component stands for a higher limit to its variability, however, it is hard to believe that this kind of signal can get more variable than when it was produced at the source; transport is always expected to dilute and smooth it. The last row in Table 3, which gives the parameters of the fitting curves through these estimates, confirms that we could reproduce the trend measured at Lut-jewad by considering the peculiar Dutch fuel mix, but we keep missing the amplitude by overestimating the variability of the tracer. We definitely cannot catch the phase of the signal measured at Lutjewad.

This example demonstrates the non-trivial effect of the terrestrial human component on APO. Of course, the effect becomes the larger the closer we get to the continents and to the anthropogenic sources. The effect could be accounted for by using a new tracer APO* defined as follows, keeping in mind that Φ (and thus also $\Phi - \beta$) has a spatial as well as a seasonal variability:

$$\Delta APO^* = \Delta APO - (\phi - \beta) \times \Delta F = \Delta O_2 + \beta \times \Delta CO_2 - (\phi - \beta) \times f(t) \times \Delta CO_2 \qquad (7)$$

Here f is the fraction of the atmospheric CO_2 mixing ratio originating from industrial processes. It could be determined e.g. by radiocarbon analysis or by CO mixing ratio measurements (e.g. Gamnitzer, 2006; Levin et al., 2008; Levin and Karstens, 2007; Meijer et al., 1996). Therefore, APO* represents a fully observation-based tracer isolating an oceanic signal.

5 Conclusions

The analysis of this data set gives new insights into the CO_2 exchange processes occurring regionally in Europe, by showing seasonal variations over 5 years, in both

the atmospheric O_2 and CO_2 mixing ratios as measured from the costal stations of Lutjewad and Mace Head. In the period from mid-2001 until mid-2005, we see an average increase of CO_2 in the atmosphere of $(1.7\pm0.2)\,\mu\text{mol}^*(\text{mol dry air})^{-1}\,\text{year}^{-1}$, and a corresponding decrease of the airborne O_2 fraction of $(-20\pm2)\,\text{per meg year}^{-1}$,

5 mainly caused by human activities, particularly fossil fuel burning. The major feature in the records is the acceleration of the airborne oxygen uptake. This acceleration must be caused by an O_2 sink up to now not accounted for. Two mechanisms have recently been proposed in the literature (Ciais et al., 2007; Randerson et al., 2006). The O_2 trend acceleration started during or shortly after the anomalously hot and dry summer

10 in Europe of 2003. A relation between both is, however, still speculative.

A climatology of the two species has also been derived. The seasonal cycles are influenced by the location of the two sampling sites more than the inter-annual long trends, with dampened amplitudes registered at Mace Head as effect of the marine character of this sampling station. Here the difference between the CO_2 summer trough

15 and the winter peak is $(14.4\pm0.3)\,\mu\text{mol}^*(\text{mol dry air})^{-1}$, while the opposite variation in the O_2 signal equals (113 ± 3) per meg. Almost half of the latter variation is due to marine processes as indicated by the APO climatology, derived for this station. At Lutjewad the CO_2 and O_2 peak-to-peak amplitudes are $(16.1\pm0.4)\,\mu\text{mol}^*(\text{mol dry air})^{-1}$ and (153 ± 3) per meg, respectively.

20 From the analysis of the Lutjewad time series, we learned that the seasonal variation of APO can be strongly influenced by processes different from those related to marine fluxes alone. A component of this APO seasonality, in an attenuated way also present in the Mace Head record, is caused by the seasonality of fossil fuel consumption and the associated mean oxidative ratio. This component needs to be taken into

25 account in the model simulations as could be shown here by the excellent agreement between the measurements and the model data when applying the OR of the actual regional fossil fuel mix. Therefore, more data on the anthropogenic emission fields are needed, both spatially and temporarily resolved. Alternatively, we propose to find another tracer capable to test models simulating transport of oceanic components over

O_2 and CO_2 observations at Lutjewad and Mace Head 2000–2005

C. Sirignano et al.

the continents. We suggest to examine a tracer APO*, similar to APO, but including a correction for all fossil fuel contributions as well. Extra input, in the form of fossil fuel CO_2 measurements, is therefore needed. Radiocarbon measurements, eventually supplemented by CO mixing ratio measurements with high time-resolution, could help to detect the fossil fuel fraction of the airborne CO_2. This kind of observations is often associated to CO_2 and O_2 records (for example in the CarboEurope IP network, cf. http://www.carboeurope.org) and they could, therefore, help to remove the residual anthropogenic component from the APO derivation.

References

Balkanski, Y., Monfray, P., Battle, M., and Heimann, M.: Ocean primary production derived from satellite data: An evaluation with atmospheric oxygen measurements, Global Biogeochem. Cy., 13, 257–271, 1999.

Battle, M., Bender, M. L., Tans, P. P., White, J. W. C., Ellis, J. T., Conway, T., and Francey, R. J.: Global carbon sinks and their variability inferred from atmospheric O_2 and δ13C, Science, 287, 2467–2470, 2000.

Battle, M., Fletcher, S. M., Bender, M. L., Keeling, R. F., Manning, A. C., Gruber, N., Tans, P. P., Hendricks, M. B., Ho, D. T., Simonds, C., Mika, R., and Paplawsky, B.: Atmospheric Potential Oxygen: New observations and their implications for some atmospheric and oceanic models, Global Biogeochem. Cy., 20, GB1010, doi:10.1029/2005GB002534, 2006.

Bender, M., Ellis, T., Tans, P., Francey, R., and Lowe, D.: Variability in the O_2/N_2 ratio of southern hemisphere air, 1991–1994: Implications for the Carbon cycle, Global Biogeochem. Cy., 10, 9–21, 1996.

Bender, M. L., Tans, P. P., Ellis, J. T., Orchardo, J., and Habfast, K.: A high-precision isotope ratio mass spectrometry method for measuring the O_2/N_2 ratio of air, Geochim. Cosmochim. Ac., 58, 4751–4758, 1994.

Bousquet, P., Gaudry, A., Ciais, P., Kazan, V., Monfray, P., Simmonds, P. G., Jennings, S. G., and O'Connor, T. C.: Atmospheric CO_2 concentration variations recorded at Mace Head, Ireland from 1992 to 1994, Phys. Chem. Earth, 21, 477–481, 1996.

BP Statistical Review of World Energy June 2008, BP p.l.c., London, UK (also available from http://www.bp.com/statisticalreview), 2008.

Ciais, P., Tans, P. P., White, J. W. C., Trolier, M., Francey, R. J., Berry, J. A., Randall, D. R., Sellers, P. J., Collatz, J. G., and Schimel, D. S.: Partitioning of ocean and land uptake of CO_2 as inferred by δ13C measurements from the NOAA Climate Monitoring and Diagnostics Laboratory Global Air Sampling Network, J. Geophys. Res., 100, 5051–5070, 1995.

Ciais, P., Reichstein, M., Viovy, N., Granier, A., Ogée, J., Allard, V., Aubinet, M., Buchmann, N., Bernhofer, C., Carrara, A., Chevallier, F., De Noblet, N., Friend, A. D., Friedlingstein, P., Grünwald, T., Heinesch, B., Keronen, P., Knohl, A., Krinner, G., Loustau, D., Manca, G., Matteucci, G., Miglietta, F., Ourcival, J. M., Papale, D., Pilegaard, K., Rambal, S., Seufert, G., Soussana, J. F., Sanz, M. J., Schulze, E. D., Vesala, T., and Valentini, R.: Europe-wide reduction in primary productivity caused by the heat and drought in 2003, Nature, 437, 529–533, 2005.

Ciais, P., Manning, A. C., Reichstein, M., Zaehle, S., and Bopp, L.: Nitrification amplifies the decreasing trends of atmospheric oxygen and implies a larger land carbon uptake, Global Biogeochem. Cy., 21, GB2030, doi:10.1029/2006GB002799, 2007.

Cleveland, R. B., Cleveland, W. S., McRae, J. E., and Terpenning, I.: STL: A seasonal-trend decomposition procedure based on Loess, Journal of Official Statistics, 6, 3–73, 1990.

Denning, A. S., Takahashi, T., and Friedlingstein, P.: Keynote perspective. Can a strong atmospheric CO_2 rectifier effect be reconciled with a "reasonable" Carbon budget?, Tellus B, 51, 249–253, 1999.

Derwent, R. G., Ryall, D. B., Manning, A. J., Simmonds, P. G., O'Doherty, S., Biraud, S., Ciais, P., Ramonet, M., and Jennings, S. G.: Continuous observations of carbon dioxide at Mace Head, Ireland from 1995 to 1999 and its net European ecosystem exchange, Atmos. Environ., 36, 2799–2807, 2002.

Friedrich, R., Freibauer, A., Gallmann, E., Giannouli, M., Koch, D., Peylin, P., Pye, S., Riviere, E., San Jose, R., Winiwarter, W., Blank, P., Kühlwein, J., Pregger, T., Reis, S., Scholz, Y., Th-

eloke, J., and Vabitsch, A.: Temporal and spatial resolution of greenhouse gas emissions in Europe, Report of a Carbo Europe workshop held at Stuttgart, Germany, 26–27 June 2003, 36 pp., 2003.

Gamnitzer, U., Karstens, U., Kromer, B., Neubert, R. E. M., Meijer, H. A. J., Schroeder, H., and Levin, I.: Carbon monoxide: A quantitative tracer for fossil fuel CO_2, J. Geophys. Res., 111, D22302, doi:10.1029/2005JD006966, 2006.

Garcia, H. E., and Keeling, R. F.: On the global oxygen anomaly and air-sea flux, J. Geophys. Res. Atmos., 106, 31155–31166, 2001.

Gloor, M., Gruber, N., Hughes, T. M. C., and Sarmiento, J. L.: Estimating net air-sea fluxes from ocean bulk data: Methodology and application to the heat cycle, Global Biogeochem. Cy., 15, 767–782, 2001.

Gruber, N., Gloor, M., Fan, S.-M., and Sarmiento, J. L.: Air-sea flux of oxygen estimated from bulk data: Implications for the marine and atmospheric oxygen cycles, Global Biogeochem. Cy., 15, 783–803, 2001.

IPCC: Climate Change 2007: The Physical Science Basis, in: Contribution of Working Group I to the Fourth Assessment Report of the Intergovernmental Panel on Climate Change, edited by: Solomon, S., Qin, D., Manning, M., Chen, Z., Marquis, M., Averyt, K. B., Tignor, M., and Miller, H. L., Cambridge University Press, Cambridge, United Kingdom and New York, NY, USA, 996 pp., 2007.

Keeling, C. D. and Whorf, T. P.: Atmospheric CO_2 records from sites in the SIO air sampling network. In Trends: A Compendium of Data on Global Change. Carbon Dioxide Information Analysis Center, Oak Ridge National Laboratory, US Department of Energy, Oak Ridge, Tenn., USA, 2005.

Keeling, R. F., Najjar, R., Bender, M., and Tans, P. P.: What atmospheric oxygen measurements can tell us about the global carbon cycle, Global Biogeochem. Cy., 7, 37–67, 1993.

Keeling, R. F.: Development of an interferometric oxygen analyzer for precise measurement of atmospheric O_2 mole fraction, PhD Thesis, Harvard University, USA, 1988.

Keeling, R. F. and Shertz, S. R.: Seasonal and interannual variations in atmospheric oxygen and implications for the global carbon cycle, Nature, 358, 723–727, 1992.

Keeling, R. F., Piper, S. C., and Heimann, M.: Global and hemispheric CO_2 sinks deduced from changes in atmospheric O_2 concentration, Nature, 381, 218–221, 1996.

Keeling, R. F., Stephens, B. B., Najjar, R. G., Doney, S. C., Archer, D., and Heimann, M.: Seasonal variations in the atmospheric O_2/N_2 ratio in relation to the kinetics of air-sea gas

Title Page

Abstract | Introduction

Conclusions | References

Tables | Figures

|◄ | ►|

◄ | ►

Back | Close

Full Screen / Esc

Printer-friendly Version

Interactive Discussion

exchange, Global Biogeochem. Cy., 12, 141–163, 1998.

Langenfelds, R. L., Francey, R. J., Steele, L. P., Battle, M., Keeling, R. F., and Budd, W. F.: Partitioning of the global fossil CO_2 sink using a 19-year trend in atmospheric O_2, Geophys. Res. Lett., 26, 1897–1900, 1999.

5 Le Quéré, C., Aumont, O., Bopp, L., Bousquet, P., Ciais, P., Francey, R., Heimann, M., Keeling, C. D., Keeling, R. F., Kheshgi, H., Peylin, P., Piper, S. C., Prentice, I. C., and Rayner, P. J.: Two decades of ocean CO_2 sink and variability, Tellus B, 55, 649–656, 2003.

Le Quéré, C., Rödenbeck, C., Buitenhuis, E. T., Conway, T. J., Langenfelds, R., Gomez, A., Labuschagne, C., Ramonet, M., Nakazawa, T., Metzl, N., Gillett, N., and Heimann, M.: Sat-
10 uration of the Southern Ocean CO_2 sink due to recent Climate Change, Science, 316, 5832, doi:10.1126/science.1136188, 2007.

Levin, I., Hammer, S., Kromer, B., and Meinhardt, F.: Radiocarbon observations in atmospheric CO_2: Determining fossil fuel CO_2 over Europe using Jungfraujoch observations as background, Sci. Total Environ., 391, 211–216, 2008.

15 Levin, I. and Karstens, U.: Inferring high-resolution fossil fuel CO_2 records at continental sites from combined 14CO_2 and CO observations, Tellus B, 59, 245–250, 2007.

Levitus, S., Antonov, J. I., Boyer, T. P., and Stephens, C.: Warming of the world ocean, Science, 287, 2225–2229, 2000.

Manning, A. C., Keeling, R. F., Katz, L. E., Paplawsky, W. J., and McEvoy, E. M.: Interpreting
20 the seasonal cycles of atmospheric oxygen and carbon dioxide concentrations at American Samoa Observatory, Geophys. Res. Lett., 30, 1333, doi:10.1029/2001GL014312, 2003.

Manning, A. C. and Keeling, R. F.: Global oceanic and land biotic carbon sinks from the Scripps atmospheric oxygen flask sampling network, Tellus B, 58, 95–116, 2006.

Marland, G., Boden, T. A., and Andres., R. J.: Global, regional, and national CO_2 emissions,
25 In Trends: A Compendium of Data on Global Change. Carbon Dioxide Information Analysis Center, Oak Ridge National Laboratory, US Department of Energy, Oak Ridge, Tenn., USA, 2005.

Meijer, H. A. J., Smid, H. M., Perez, E., and Keizer, M. G.: Isotopic characterisation of anthropogenic CO_2 emissions using isotopic and radiocarbon analysis, Phys. Chem. Earth, 21,
30 483–487, 1996.

Nakazawa, T., Ishizawa, M., Higuchi, K., and Trivett, N. B. A.: Two curve fitting methods applied to CO_2 flask data, Environmetrics, 8, 197–218, 1997.

Neubert, R. E. M., Spijkervet, L. L., Schut, J. K., Been, H. A., and Meijer, H. A. J.: A computer-

controlled continuous air drying and flask sampling system, J. Atmos. Ocean. Tech., 21, 651–659, 2004.

Neubert, R. E. M., Weber, P., Gerritsma, R., and Meijer, H. A. J.: The Atmospheric CO_2 and greenhouse gas monitoring activities at Lutjewad, The Netherlands, in: Report of the twelfth WMO/IAEA meeting of experts on Carbon Dioxide concentration and related tracer measurement techniques, Toronto, Canada, 15–18/9/2003, edited by: Worthy, D. and Huang, L., WMO-TD No. 1275, WMO-GAW No.161, 203–209, Geneve, Switzerland, 2005.

Olivier, J. G. J. and Berdowski, J. J. M.: Global emission sources and sinks., in: The climate system, edited by: Berdowski, J., Guicherit, R., and Heij, B. J., A. A. Balkema Publishers/Swets & Zeitlinger Publishers, Lisse, The Netherlands, 33–78, 2001.

Press, W. H., Flannery, B. P., Teukolsky, S. A., and Vetterling, W. T.: General linear least squares fit, in: Numerical recipes in C: The art of scientific computing, Cambridge University Press, Cambridge, UK, 671–681, 1992.

Randerson, J. T., Masiello, C. A., Still, C. J., Rahn, T., Poorter, H., and Field, C. B.: Is carbon within the global terrestrial biosphere becoming more oxidized? Implications for trends in atmospheric O_2, Glob. Change Biol., 12, 260–271, 2006.

Raupach, M. R., Marland, G., Ciais, P., Le Quéré, C., Canadell, J. G., Klepper, G., and Field, C. B.: Global and regional drivers of accelerating CO_2 emissions, P. Natl. Acad. Sci. USA, 104, 10 288–10 293, doi:10.1073/pnas.0700609104, 2007.

Rayner, P. J., Enting, I. G., Francey, R. J., and Langenfelds, R. L.: Reconstructing the recent carbon cycle from atmospheric CO_2, $\delta^1 3C$ and O_2/N_2 observations, Tellus B, 51, 213–232, 1999.

Rödenbeck, C.: Estimating CO_2 sources and sinks from atmospheric mixing ratio measurements using a global inversion of atmospheric transport, Max-Planck-Institute for Biogeochemistry, Technical Reports Nr. 6, Jena, Germany, 53 pp., ISSN 1615–7400, 2005.

Schmidt, M., Graul, R., Sartorius, H., and Levin, I.: Carbon dioxide and methane in continental Europe: a climatology and ^{222}Radon-based emission estimates, Tellus B, 48, 457–473, 1996.

Severinghaus, J. P.: Studies of the terrestrial O_2 and Carbon Cycles in sand dune gases and in Biosphere 2, PhD Thesis, Columbia University, New York, 148 pp., 1995.

Stephens, B. B., Keeling, R. F., Heimann, M., Six, K. D., Murnane, R., and Caldeira, K.: Testing global ocean carbon models using measurements of atmospheric O_2 and CO_2 concentration, Global Biogeochem. Cy., 12, 213–230, 1998.

O_2 and CO_2 observations at Lutjewad and Mace Head 2000–2005

C. Sirignano et al.

Stephens, B. B.: Field-based atmospheric oxygen measurements and the ocean carbon cycle, PhD Thesis, University of California, San Diego, 221 pp., 1999.

Stephens, B. B., Bakwin, P. S., Tans, P. P., Teclaw, R. M., and Baumann, D. D.: Application of a differential fuel-cell analyzer for measuring atmospheric oxygen variations, J. Atmos. Ocean. Tech., 24, 82–94, 2007.

Sturm, P., Leuenberger, M., Sirignano, C., Neubert, R. E. M., Meijer, H. A. J., Langenfelds, R. L., Brand, W. A., and Tohjima, Y.: Permeation of atmospheric gases through polymer O-rings used in flasks for air sampling, J. Geophys. Res., 109, D04309, doi:10.1029/2003JD004073, 2004.

Sturm, P., Leuenberger, M., Moncrieff, J., and Ramonet, M.: Atmospheric O_2, CO_2 and δ13C measurements from aircraft sampling over Griffin Forest, Perthshire, UK, Rapid Commun. Mass Sp., 19, 2399–2406, 2005a.

Sturm, P., Leuenberger, M., and Schmidt, M.: Atmospheric O_2, CO_2 and $\delta^1$3C observations from the remote sites Jungfraujoch, Switzerland, and Puy de Dôme, France, Geophys. Res. Lett., 32, L17811, doi:10.1029/2005GL023304, 2005b.

Sturm, P., Leuenberger, M., Valentino, F. L., Lehmann, B., and Ihly, B.: Measurements of CO_2, its stable isotopes, O_2/N_2, and ^{222}Rn at Bern, Switzerland, Atmos. Chem. Phys., 6, 1991–2004, 2006,
http://www.atmos-chem-phys.net/6/1991/2006/.

Takahashi, T., Sutherland, S. C., Sweeney, C., Poisson, A., Metzl, N., Tilbrook, B., Bates, N., Wanninkhof, R., Feely, R. A., and Sabine, C.: Global sea-air CO_2 flux based on climatological surface ocean $p CO_2$, and seasonal biological and temperature effects, Deep Sea Res. Pt II, 49, 1601–1622, 2002.

Tans, P. P., Conway, T. J., and Nakazawa, T.: Latitudinal distribution of the sources and sinks of atmospheric carbon dioxide derived from surface observations and an atmospheric transport model, J. Geophys. Res., 92, 5151–5172, 1989.

Tans, P. P., Fung, I. Y., and Takahashi, T.: Observational constraints on the global atmospheric CO_2 budget, Science, 247, 1431–1438, 1990.

Valentino, F. L., Leuenberger, M., Uglietti, C., and Sturm, P.: Measurements and trend analysis of O_2, CO_2 and δ^{13}C of CO_2 from the high altitude research station Junfgraujoch, Switzerland – A comparison with the observations from the remote site Puy de Dôme, France, Sci. Total Environ., 391, 203–210, 2008.

Title Page

Abstract | Introduction

Conclusions | References

Tables | Figures

|◄ | ►|

◄ | ►

Back | Close

Full Screen / Esc

Printer-friendly Version

Interactive Discussion

Zhao, C. L. and Tans, P. P.: Estimating uncertainty of the WMO mole fraction scale for carbon dioxide in air, J. Geophys. Res., 111, D08S09, doi:10.1029/2005JD006003, 2006.

Table 1. Amplitude and phase parameters of the seasonal component of the fit to the observed values of CO$_2$ and O$_2$ mixing ratios at both studied stations.

	peak-to-trough amplitude	Calendar day of		±days
		min	max	
CO$_2$ Mace Head	14.4±0.3 μmol/mol	27 Aug	26 Feb	3
O$_2$ Mace Head	113±3 per meg	14 Mar	8 Sep	4
CO$_2$ Lutjewad	16.1±0.4 μmol/mol	14 Aug	7 Mar	3
O$_2$ Lutjewad	153±3 per meg	28 Mar	11 Sep	3

O_2 and CO_2 observations at Lutjewad and Mace Head 2000–2005

C. Sirignano et al.

Table 2. The trends and their variability during the studied period at both stations. Both CO_2 and O_2 trends are given in (μmol*(mol dry air)$^{-1}$ per year).

	CO_2 LUT	CO_2 MHD	O_2 LUT	O_2 MHD
Jul 2000 . . . Jul 2005	1.7±0.2	1.7±0.1	−20±1.5	−19±1.5
Jan 2002 . . . Jan 2005	1.6±0.5	1.9±0.2	−27±3	−25±4

Table 3. Parameters of the harmonic fit to the modelled and observed APO at Mace Head and Lutjewad. Amplitude and phase are taken from the curves through the monthly or bimonthly means of detrended APO data, as shown in Fig. 6.

	peak-to-trough amplitude (μmol/mol)	Trend (μmol/mol)per year	Calendar day of max
MHD observed	9.4±2	−2.1±0.4	27 Jul±12
MHD modelled	10.8±0.6	−1.85±0.07	2 Aug±4
LUT observed	14±2	−2.5±0.3	16 Aug±8
LUT modelled	8.8±0.4	−1.69±0.08	2 Aug±3
LUT mod. (modif.)	21.4±0.6	−2.5±0.11	14 Jul±2

© planiglobe.com 2008
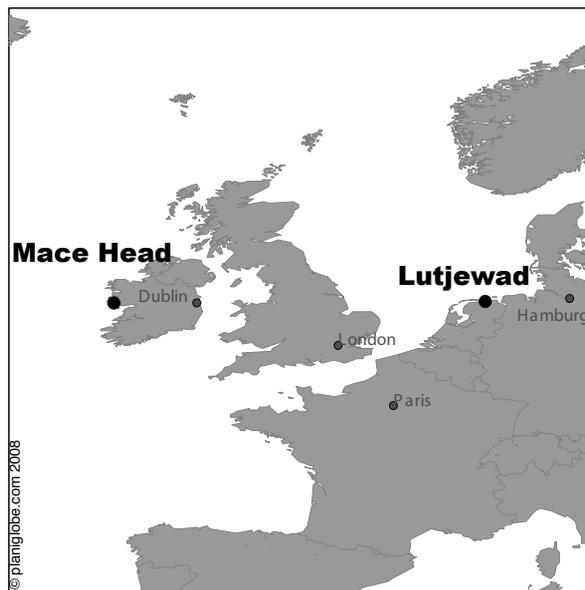
Fig. 1. The sampling sites Mace Head (MHD) and Lutjewad (LUT) in Western Europe (map produced under creative commons license by Planiglobe.com).
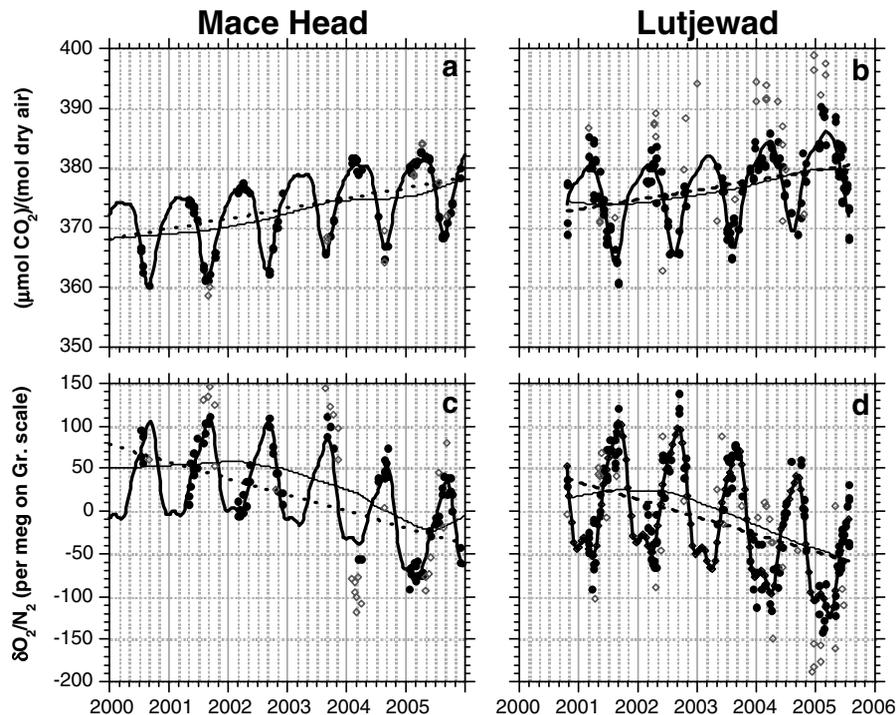
Fig. 2. Carbon dioxide **(a)**, **(b)** and oxygen **(c)**, **(d)** mixing ratio records at the stations Lutjewad (a), (c) and Mace Head (b), (d). The solid lines are a linear combination of three harmonics and a trend function, fitted through the observations. The dashed line represents the average trend while the thin grey line is the Loess component (trend) of the fit. Empty symbols are the observations considered outliers according to the procedure described in the text.
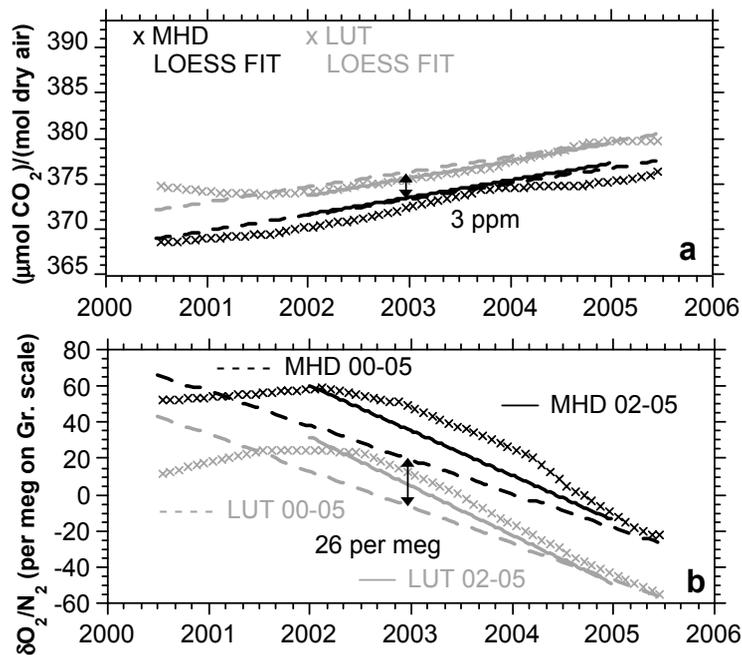
Fig. 3. The variability in the trends of CO$_2$ and O$_2$ mixing ratios trends at Mace Head and Lutjewad, according to fit procedure and period.
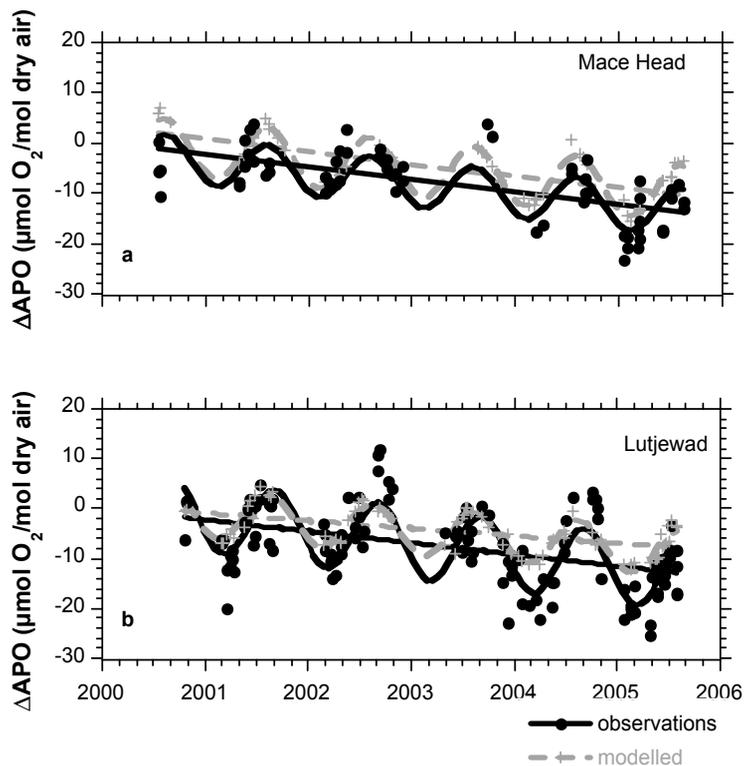
Fig. 4. APO time series at Mace Head **(a)** and Lutjewad **(b)**. Model outputs, selected at the same sampling time as the observations, are represented by grey crosses. The fit curves through the model outcomes are plotted in grey with dashed lines.
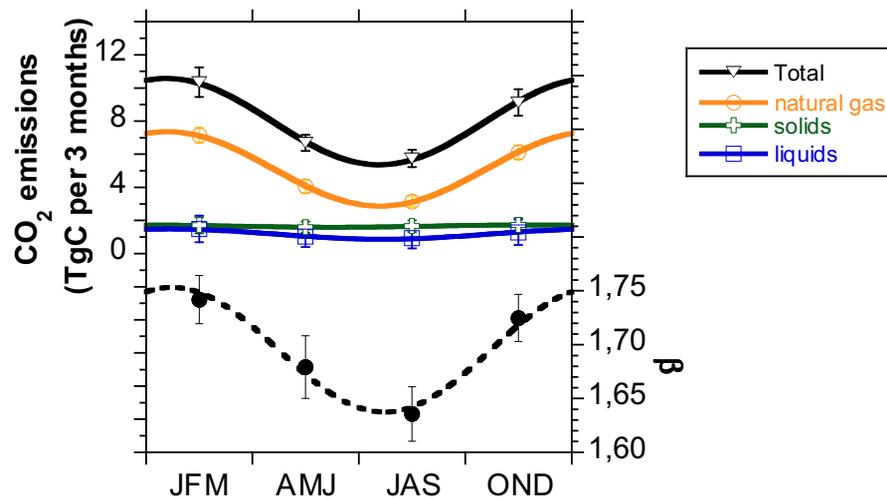
Fig. 5. The seasonality of the Dutch fossil fuel mix and of the resulting fossil fuel oxidative ratio.
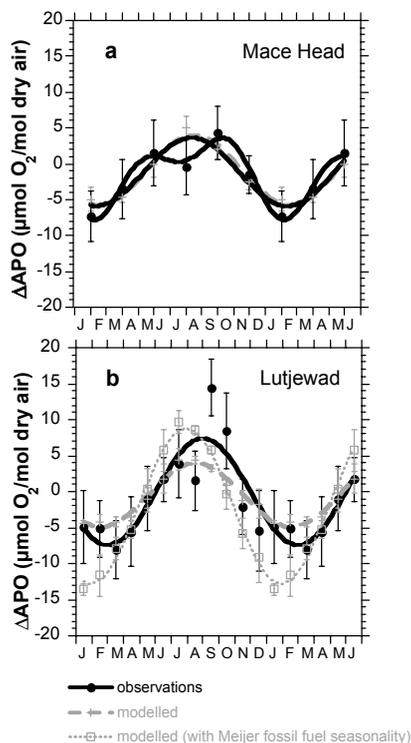
Fig. 6. APO climatology at Mace Head **(a)** and Lutjewad **(b)**. Monthly (resp. bimonthly for MHD) averages of the detrended APO are represented by black full circles at both stations and compared to model simulations in grey, which at Lutjewad take (squares) or take not (plusses) into account the seasonal variation in the actual fossil fuel mix. The observations (solid lines) and the simulations (dashed lines) are fitted by a single harmonic function. Only for Mace Head a second fitting curve containing also a second harmonic component has been plotted, to highlight the peak occurring during the months September and October at both stations, which does not appear in the model simulations.